Targeting B7-H3 through EZH2 inhibition in MYC-positive Group 3 medulloblastoma

KATHERINE SHISHIDO[1], IAN J. PURVIS[1], KIRAN K. VELPULA[1-3], SUJATHA VENKATARAMAN[4], RAJEEV VIBHAKAR[4] and SWAPNA ASUTHKAR[1,3]

Departments of [1]Cancer Biology and Pharmacology, [2]Neurosurgery, [3]Pediatrics, University of Illinois College of Medicine at Peoria, Peoria, IL 61605; [4]Department of Pediatrics, University of Colorado School of Medicine, Aurora, CO 80045, USA

Received October 19, 2022; Accepted February 20, 2023

DOI: 10.3892/or.2023.8556

Abstract. The most aggressive subtype of medulloblastoma (MB), Group 3, is characterized by MYC amplifications. However, targeting MYC has proven unsuccessful, and there remains a lack of therapeutic targets for treating MB. Studies have shown that the B7 homolog 3 (B7-H3) promotes cell proliferation and tumor cell invasion in a variety of cancers. Similarly, it was recently revealed that B7-H3 promotes angiogenesis in Group 3 MB and likely facilitates MB metastasis through exosome biogenesis. While therapies targeting B7-H3 remain in the early stages of development, targeting upstream regulators of B7-H3 expression may be more effective for halting MB progression. Notably, MYC and the enhancer of zeste homolog 2 (EZH2) are known to regulate B7-H3 expression, and a previous study by the authors suggested that B7-H3 amplifications present in MB are likely the result of EZH2-MYC mediated activities. In the present study, it was reported that overexpression of EZH2 is associated with lower overall survival in Group 3 MB patients. It was also revealed that inhibition of EZH2 significantly reduces B7-H3 and MYC transcript levels and upregulates miR-29a, indicating that EZH2 post-transcriptionally regulates B7-H3 expression in Group 3 MB cells. Pharmacological inhibition of EZH2 using EPZ005687 attenuated MB cell viability and reduced the expression of B7-H3. Similarly, pharmacological inhibition and knockdown of EZH2 led to the downregulation of MYC, B7-H3, and H3K27me3. Further, EZH2 silencing induced apoptosis and reduced colony-forming ability in MB cells, whereas EZH2 inhibition in MYC-amplified C17.2 neural stem cells induced G2/M phase arrest while downregulating B7-H3 expression. Collectively, the current study positions EZH2 as a viable target for the future development of MB treatments and that targeting EZH2 in combination with B7-H3 immunotherapy may be an effective treatment for halting MB progression.

Correspondence to: Dr Swapna Asuthkar, Department of Cancer Biology and Pharmacology, University of Illinois College of Medicine at Peoria, 1 Illini Drive, Peoria, IL 61605, USA
E-mail: asuthkar@uic.edu

Key words: medulloblastoma, B7-H3, enhancer of zeste homolog 2, Myc, EPZ005687

Introduction

Medulloblastoma (MB) is the most common malignant pediatric cancer, with ~1,800 new cases diagnosed in the United States every year (1-3). MB is classified into four distinct subgroups: Sonic hedgehog (SHH), wingless (WNT), Group 3 and Group 4 (4), with each subgroup displaying distinct clinical presentation and genomic features (5,6). Histological variants of MB are broadly classified as classic (CMB), desmoplastic/nodular (DN), MB with extensive nodularity (MBEN), and large cell/anaplastic (LC/A) (7,8). Amplification of *c-MYC* is more frequently observed in tumors with LC/A histology (9,10) and in high-risk Group 3 and SHH tumors with TP53 abnormalities (11). Notably, MYC-amplified Group 3 MBs exhibit a higher frequency of metastasis and have the worst prognosis (12,13). Unfortunately, MYC inhibition has proven unsuccessful in improving Group 3 MB patient outcomes (14). As such, it is imperative to expound on the mechanisms contributing to MB pathogenesis to identify viable targets for developing novel therapeutics.

Initial studies on B7 homolog 3 (B7-H3) in cancer primarily focused on its role in promoting immune evasion (15-17). However, B7-H3 also exerts non-immunological functions to promote tumorigenesis and metastasis (18-20). For example, in hepatocellular carcinoma and melanoma, B7-H3 stimulates cell invasion and migration (21,22), while in glioblastoma, B7-H3 promotes the epithelial-to-mesenchymal transition (23). It was recently demonstrated by the authors that B7-H3 is upregulated in Group 3 MBs and is associated with poor survival in MB patients (24). Further, it was showed that B7-H3 promotes angiogenesis and likely facilitates MB pathogenesis via the exosome biogenesis (24,25). As a result of its diverse functions, there has been increased interest in therapeutically targeting B7-H3, with B7-H3 inhibitors showing success in clinical trials (NCT01391143 and NCT02982941). For instance, enoblituzumab (MGA271) is a humanized anti-B7H3 monoclonal antibody with an engineered Fc domain that is optimized to augment antitumor effector-mediated functions (26). It accomplishes so by enhancing the binding of CD16A (FcγRIIa) to

trigger antibody-dependent cell-mediated cytotoxicity (26) and prevent the binding of CD32B (FcγRIIb), an inhibitory receptor expressed on immune cells which dampens B-cell activation and signaling (27).

In addition to B7-H3, MYC-amplified Group 3 MBs overexpress the enhancer of zeste homolog 2 (EZH2) (28). EZH2 is the enzymatic catalytic subunit of the polycomb repressive complex 2 (PRC2) (29). As a histone modifier, EZH2 is best known for repressing gene transcription through the trimethylation of H3K27 (H3K27me3) (30). Similar to MYC, EZH2 can also indirectly regulate gene expression through microRNAs (miRNAs or miRs) (31). Of particular interest is the miR-29 family, which includes miR-29a, miR-29b1/2 and miR-29c (32). For example, EZH2 directly inhibits the transcription of miR-29b to upregulate the LOXL4 expression (33). Notably, EZH2 has been shown to bind to the promoter region of miR-29a/b1 and miR29b2/c to facilitate MYC-mediated silencing of miR-29a-c expression (34). Notably, miR-29a directly binds to the 3'-untranslated region (UTR) of B7-H3 transcripts to induce translational repression (35). In a previous study by the authors, it was found that overexpression of miR-29a/b significantly reduced the protein levels of B7-H3. Further, it was showed that B7-H3 expression was recused upon MYC inhibition (24). Collectively, these observations suggested that MYC and EZH2 may regulate B7-H3 expression directly or indirectly through miR-29 inhibition.

While research has supported the therapeutic potential of B7-H3 inhibitors, such as enoblituzumab, suitable therapies against B7-H3 remain in their infancy. As such, investigating upstream regulators of B7-H3 expression may provide more immediate effective therapies. One such regulator is miR-29. However, the inability to successfully deliver miRNA-based therapies to tumors and their inherent broad functionalities impede the use of miRNA-based therapies in the clinical setting (35). Therefore, epigenetic therapies targeting EZH2 may to lead to more effective methods of suppressing B7-H3. For instance, studies have shown that Tazemetostat, a small-molecule inhibitor of EZH2, demonstrates antitumor activity in patients with advanced solid tumors (36), and has been recently approved by the FDA for the treatment of relapsed/refractory follicular lymphoma (37) (NCT01897571).

In the present study, it was reported that high expression of EZH2 is associated with lower overall survival in Group 3 MB patients. EZH2 silencing downregulated B7-H3 and MYC transcript and protein expression, while pharmacological inhibition of EZH2 significantly reduced clonogenic survival in MYC-amplified Group 3 MB cells. It was further identified that both EZH2 and B7-H3 inhibition decreased the viability of C17.2 cells stably overexpressing EZH2. Importantly, it was demonstrated that EZH2 targeting markedly increased miR-29a expression in Group 3 MB cells, suggesting that EZH2 inhibition facilitates miR-29-mediated suppression of B7-H3.

Materials and methods

Cell lines and transfection. The MB cell lines used in the present study included D425 and D458 (38), were cultured in complete DMEM media with 10% FBS, 1% penicillin/streptomycin, 1% sodium pyruvate (Gibco; Thermo Fisher Scientific, Inc.), The C17.2 and C17.2-EZH2-OE murine neural stem cells (NSC) (28) were maintained in complete DMEM media with 10% FBS, 1% penicillin/streptomycin, 1% sodium pyruvate (Gibco; Thermo Fisher Scientific, Inc.; cat. no. 15140122), and 5% equine serum (39,40). All the cells were incubated at 37˚C with 5% CO_2. D425 and D458 cells with 80% confluency were serum-starved for 30 min in 1.5 ml of serum-free media on 60-mm plates before transfection. Transfections for both cell lines were carried out using Lipofectamine® 2000 (cat. no. 11668030; Thermo Fisher Scientific, Inc.). Cells were incubated with the reagent-plasmid (2 μg) complex for 6 h, and then 1.5 ml of complete media was added for overnight incubation. The following morning, the media was replaced with complete media and incubated further for 24 h.

Plasmids, chemicals, and inhibitors. The short hairpin (sh)EZH2 plasmids were obtained from Dr Vibhakar's lab (28). B7-H3 overexpression (B7-H3-OE) plasmid was obtained from Sino Biological, Inc. (cat. no. HG11188-CY). EZH2 inhibitor (EPZ005687) was purchased from TargetMol (cat. no. T1905). MYC inhibitor (JQ1) was purchased from Cayman Chemical Company (cat. no. 11187) and anti-B7-H3 monoclonal MJ18 Ab was purchased from Bio X Cell (cat. no. BE0124).

In silico analysis. The Kaplan-Meier survival curve of all Group 3 MB patients was plotted using the Cavalli dataset within the R2 program (http://r2.amc.nl) (24). Data mining of classic, large cell, and nodular desmoplastic MB histology types was carried out using the mixed MB xenograft dataset (Zhao-92-custom-ilmnhwg6v2) available on the R2 software.

RNA isolation and reverse transcription-quantitative PCR (RT-qPCR). Total RNA was isolated using TRIZOL® reagent (Invitrogen; Thermo Fisher Scientific, Inc.). RT-qPCR was performed using CFX96 Real-Time System (BioRad Laboratories, Inc.) to analyze mRNA levels (41). The PCR reactions were run in triplicates using PowerTrack SYBR Green Master Mix (Thermo Fisher Scientific, Inc.; cat. no. A46109). ~2 μg of RNA was converted to cDNA using a cDNA synthesis kit (Bio-Rad Laboratories, Inc.). Reverse transcription was carried out for 30 min at 55˚C followed by 5 min at 85˚C. The qPCR thermocycling conditions included an initial denaturation step at 95˚C for 10 min, followed by 40 cycles of denaturation at 95˚C for 10 sec and annealing at 60˚C for 30 sec. The expression level of the target genes was normalized to Actin and the fold change was calculated using the $2^{-\Delta\Delta Cq}$ method. The primer sequences used, including controls, are listed in the Table SI (24,42,43).

Western blotting. For western blots, cells were lysed in 1X RIPA buffer (cat. no. J62725-AP; Thermo Fisher Scientific, Inc.) containing protease inhibitor cocktail (cat. no. 11697498001; Roche Diagnostics). Cell lysates were sonicated, 4x30 sec with 30 sec intervals between each sonication, and centrifuged at 20,817 x g for 15 min at 4˚C. Supernatants were collected for protein estimation as determined by BCA (cat. no. A53225; Thermo Fisher Scientific, Inc.). Equal concentrations of cell lysates (40 μg per load) were resolved by SDS-PAGE, and western blot analysis was performed using nitrocellulose membrane and specific antibodies. EZH2 and B7-H3

were run on 10% SDS gels, 12% SDS gels were used for MYC and 15% gels were used to visualize H3K27me3. For H3K27me3, separate gels were run for actin, using 10% gel; the lysates and concentrations were unchanged. Blocking for all blots was performed using 10% non-fat milk for 1 h at room temperature. After which, the blots were treated with primary antibody at 4˚C for overnight followed by secondary antibody for 1 h at room temperature. Mouse polyclonal antibodies against B7-H3 (1:1,000; cat. no. sc-376769; Santa Cruz Biotechnology, Inc.) (44) and c-MYC (1:1,000; cat. no. sc-40; Santa Cruz Biotechnology, Inc.) (45) and rabbit polyclonal antibodies against EZH2 (1:1,000; cat. no. 4905; Cell Signaling Technology, Inc.) (46) and H3K27me3 (1:1,000; cat. no. sc-56616; Santa Cruz Biotechnology, Inc.) (47), were used as primary antibodies. With the exception of H3K27me3, all blots presented in the manuscript were stripped and incubated with anti-β-actin (1:10,000; cat. no. 3700; Cell Signaling Technology, Inc.) (48) as the loading control. Anti-mouse/rabbit IgG HRP conjugated antibody (1:10,000; cat. no. 400111; Novus Biologicals, LLC) was used as a secondary antibody. Immunodetection was accomplished using ECL reagents (cat. no. 1705060S; BioRad Laboratories, Inc). Densitometric analysis was carried out using ImageJ software (version 1.53t 24; National Institutes of Health).

3-(4,5-dimethylthiazol-2-yl)-2,5-diphenyltetrazoliumbromide (MTT) assay. Cell viability was determined by MTT assays (cat. no. M5655-100MG; MilliporeSigma). D425 and D458 cell lines were seeded in 96-well plates at a concentration of $5x10^3$ cells/well. The C17.2 and C17.2-EZH2-OE cell lines were seeded in 96-well plates at a concentration of $3x10^3$ cells/well. The D425 and D458 cell lines were treated with increasing concentrations of EPZ005687 (0, 10, 20, 40 and 80 μM) for 5 days. C17.2 and C17.2-EZH2-OE cell lines were treated with increasing concentrations of EPZ005687 (0, 10, 15, 20, 25, 30 and 40 μM), IgG (0, 2.5, 5 and 10 μg), or MJ18 (0, 2.5, 5, 10 μg) for 5 days. After treatment, the medium was replaced with 100 μl sterile MTT solution (cat. no. M6494; Thermo Fisher Scientific, Inc.) per well (0.5 μg/ml), and cells were incubated for 2 h in a cell culture incubator at 37˚C. The MTT crystals were solubilized in DMSO (cat. no. D8418; MilliporeSigma) for 30 min. Absorbance was read using a SpectraMax M5 spectrophotometer (Molecular Devices, LLC) at 550 nm.

Phycoerythrin (PE) staining, cell cycle analysis and clonogenic assay. For PE staining, D425 cells were cultured in 100-mm dishes to 80% confluency. A total of 24 h after inoculation, the cells were randomized and treated with JQ1 (1 μM) or EPZ005687 (20 μM) for 24 h. Harvested cells were fixed in ice-cold (-20˚C) 70% ethanol overnight. Cells were then washed twice with 1X PBS and labeled with 5 μl (0.25 μg/million cells) PE anti-human CD276 (B7-H3) antibody (cat. no. 331605; BioLegend, Inc.). For the cell cycle analysis, D425, D458, C17.2 and C17.2 EZH2-OE cells ($1x10^6$, n=4) were seeded in 60-mm plates. After 24 h, the media was removed and replaced with media alone (control), JQ1 (1 μM), or EPZ005687 (20 μM) and incubated further for 24 h. Cells were harvested, washed with 1X PBS, and then fixed in 1 ml ice cold 70% ethanol at -20˚C overnight. Fixed cells were then washed with PBS and resuspended in 500 μl of propidium iodide staining solution (50 μg/ml) (cat. no. 1032; BioSure). The cell cycle was analyzed by FACS Caliber System (Becton Dickinson and Company) following standard protocol (49). The proportion of cells in each phase of the cell cycle was assessed using Cell Quest software (Becton, Dickinson and Company). For the clonogenic assay (colony formation assay), D425 and D458 cells were seeded in 60-mm plates at 50 and 100 cells for 24 h. After which, the cells were treated with JQ1 (1 μM) or EPZ005687 (20 μM). The cells were allowed to form colonies over a period of 14 days. Colonies were measured as a cluster of 50 or more cells. Media and inhibitor treatments were changed every three days. Colonies were fixed with 4% paraformaldehyde for 20 min and stained using crystal violet (0.5%) overnight. The samples were then quantified by manual inspection.

Statistical analysis. Statistical analysis and graphing were performed using Origin version 9.0 software (Microcal Software Inc.). Statistical significance for independent samples was calculated using one-way ANOVA with Tukey's post hoc test. Data are expressed as the median ± SD. $P<0.05$ was considered to indicate a statistically significant difference.

Results

High EZH2 expression is associated with poor prognosis in Group 3 MB patients. B7-H3 levels are significantly elevated in patients with hepatocellular carcinoma, non-small cell lung cancer, renal cell carcinoma and osteosarcoma, with greater levels of B7-H3 associated with higher tumor stage, tumor size, and metastasis status (50-52). Similarly, EZH2 expression increases with tumor grade and is associated with poor patient prognosis (53), prompting interest in targeting epigenetic modifiers such as EZH2 in MB (53,54). As previously revealed, B7-H3 amplifications are associated with reduced survival in MB patients (24). Previous studies suggested that EZH2 may regulate B7-H3 expression (34,55), thus the expression of EZH2 and B7-H3 in Group 3 MB patient survival was compared by data mining using the publicly available MB patient datasets. Kaplan-Meier survival curves plotted using the Cavalli dataset revealed a significant association between Group 3 MB patients with high EZH2 expression (n=84) and poor overall survival when compared with patients with low EZH2 expression (n=29, $P<0.001$). Similarly, MB patients with high B7-H3 expression (n=84) had lower overall survival when compared with patients with low B7-H3 expression (n=29, $P<0.05$) (Fig. 1A), highlighting the clinical significance of targeting EZH2 in MYC amplified Group 3 MB. To further identify the relationship among EZH2, B7-H3, and MYC transcript expression in MB, a data mining analysis (https://hgserver1.amc.nl/cgi-bin/r2/main.cgi) of xenografts representative of different MB histological variants was performed; classic (n=14), large cell (n=8) and desmoplastic/nodular (n=18) (Fig. 1B). For this analysis, the relative transcript levels among EZH2, B7-H3 and MYC in the different MB histological variants were compared by their respective Z score. Similar to Group 3 MB, the large cell/anaplastic MB variant is frequently associated with MYC amplification (9,10,56,57). In agreement with previous studies, the present analysis showed that both EZH2 and MYC transcript levels were highly expressed in

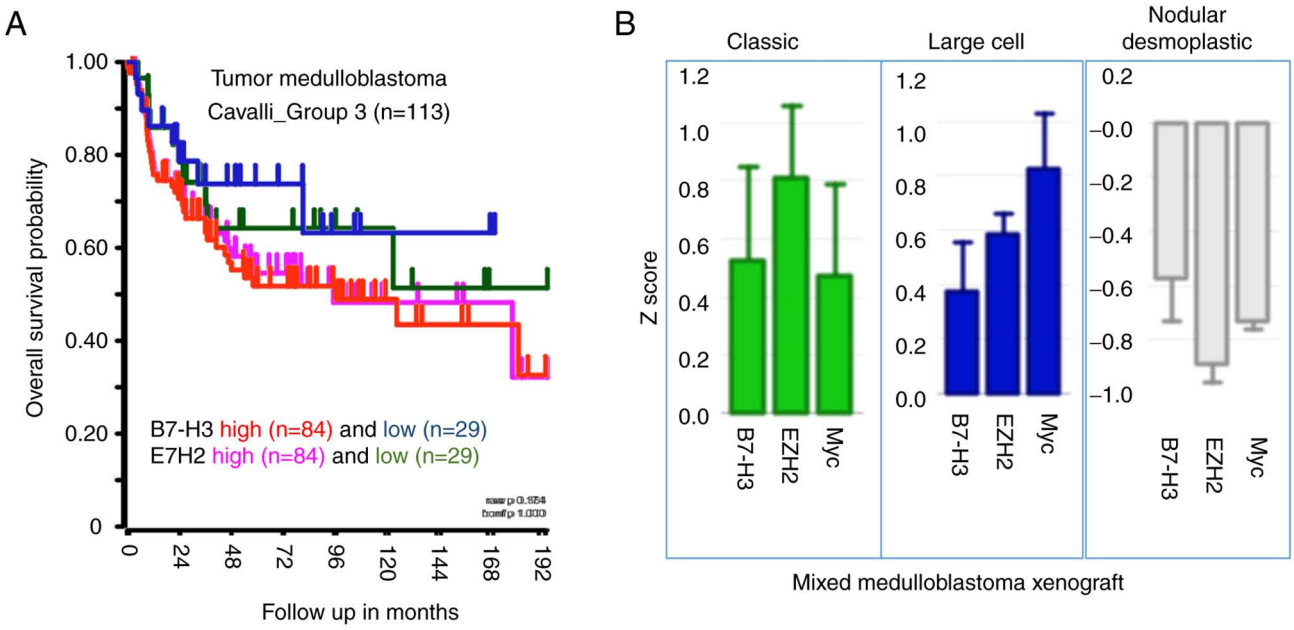

Figure 1. High EZH2 expression is associated with poor prognosis in Group 3 MB patients. (A) Kaplan-Meier analysis of Group 3 MB patients showing the association between OS and EZH2 and B7-H3 expression. The data presented does not take into consideration MYC amplification. The results indicated that Group 3 MB patients with either high expression of EZH2 (n=84, pink) and B7-H3 (n=84, red) had significantly lower OS than patients with low EZH2 (n=29, green) and B7-H3 (n=29, blue). (B) Bar plot representing B7-H3, EZH2 and MYC transcript levels in classic (n=14), large cell (n=8), and nodular desmoplastic (n=18) MB samples. The mixed medulloblastoma xenograft dataset (Zhao-92-custom-ilmnhwg6v2) available on the R2 software was used for data mining. EZH2, enhancer of zeste homolog 2; MB, medulloblastoma; OS, overall survival.

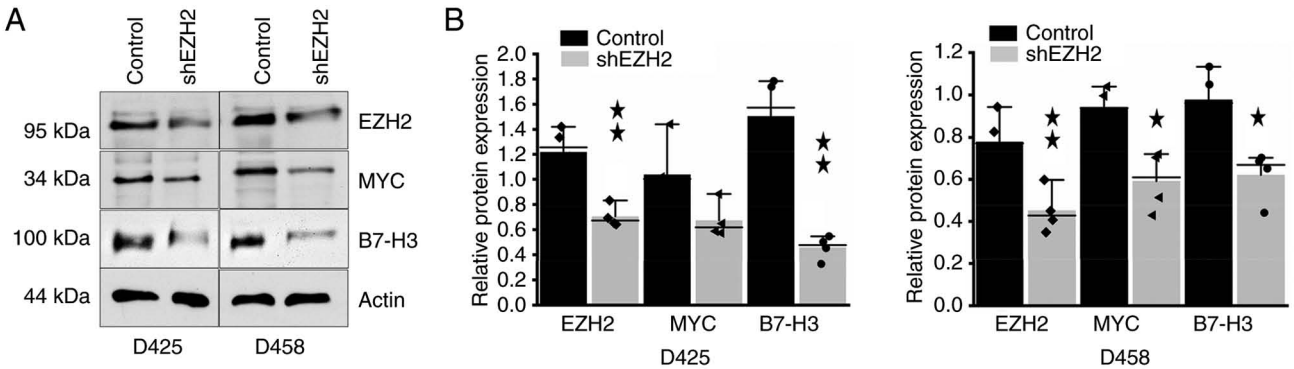

Figure 2. Association among B7-H3, EZH2 and MYC in MB. (A) Immunoblot of EZH2, MYC and B7-H3 protein expression (40 μg) in control and shEZH2 transfected D425 and D458 cells. Cells were transfected for 48 h prior to analysis. All blots were stripped and incubated with actin as the loading control. (B) Scatterplot bar graph of EZH2, MYC and B7-H3 protein expression in control and shEZH2-transfected MB cells. The horizontal black bar represents the median. The vertical black bar represents the SD. *P<0.05 and **P<0.01. EZH2, enhancer of zeste homolog 2; MB, medulloblastoma; sh-, short hairpin.

both classic and large cell MB variants (58,59). By contrast, nodular desmoplastic MB xenografts exhibited lower EZH2, MYC and B7-H3 transcript levels.

EZH2 silencing reduces B7-H3 and MYC expression. Targeting MYC and miR-29 reduces B7-H3 expression in MB cells (24), yet clinical translational studies of drugs targeting MYC and miRNAs have proven unsuccessful (35,60-62). As a result, EZH2 inhibition has become an attractive alternative approach for suppressing B7-H3 expression, particularly in MB (63,64). To determine whether EZH2 affects B7-H3 expression at the translational level, immunoblot analysis of D425 and D458 cells transfected with shRNA targeting EZH2 (shEZH2) was performed (65). Statistical analysis revealed that B7-H3 protein expression was downregulated in D425 (P<0.01) and D458 (P<0.05) cell lines transfected with shEZH2 plasmids. Further, EZH2 depletion downregulated MYC protein expression in D425 and D458 cells (Fig. 2A and B).

Pharmacological inhibition of EZH2 is cytotoxic to MB cells and downregulates B7-H3. EZH2 has been shown to prolong cell survival in a variety of cancers (66). As the proliferative effects of EZH2 silencing have been studied in MB, both *in vitro* and *in vivo* (28,65), it was sought to determine the impact of EZH2 inhibition using EPZ005687 on MB cell viability by MTT assay. EZP005687 was chosen as it directly targets PRC2 enzymatic activity with high selectivity when compared with more traditional EZH2 inhibitors (67,68). The

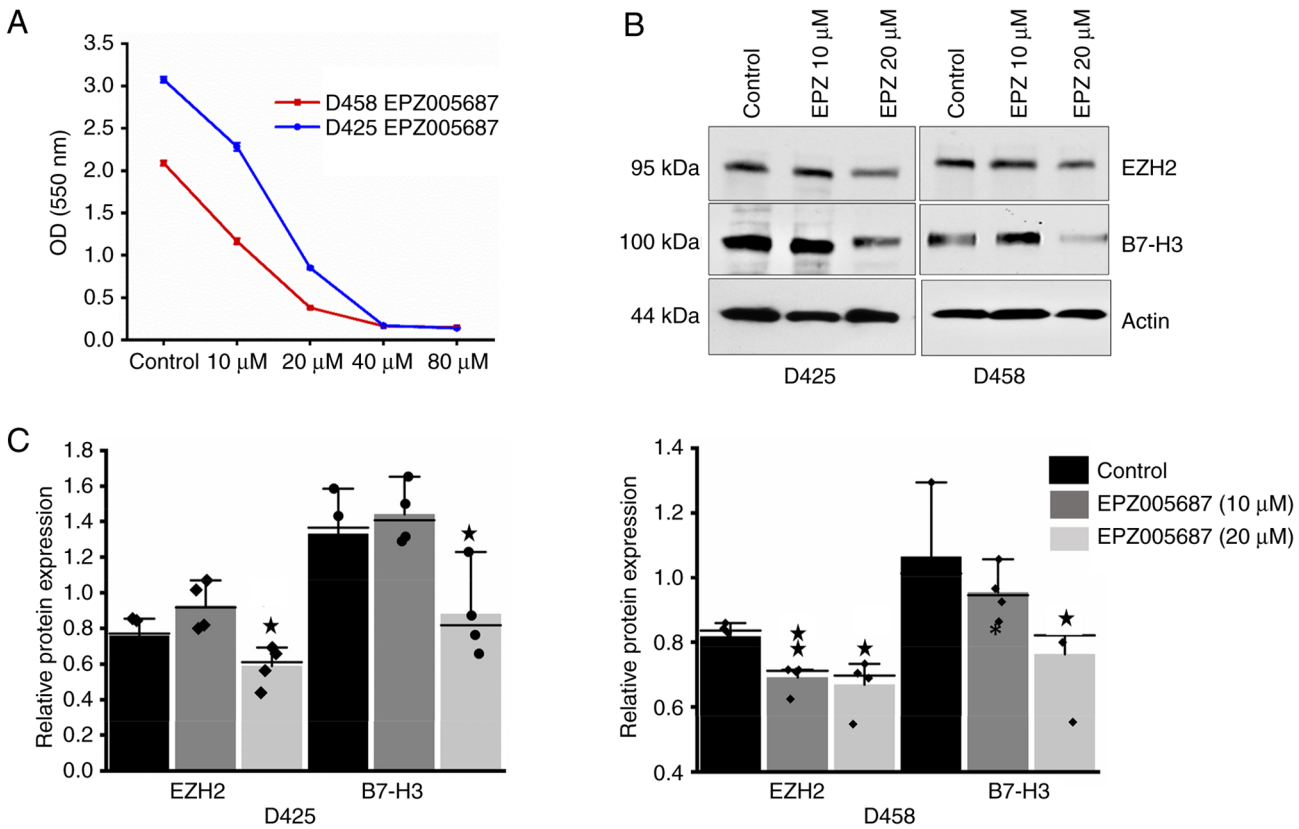

Figure 3. EZH2 inhibition impairs MB cell viability and downregulates B7-H3 expression. (A) MTT assay of D425 and D458 cells treated with increasing concentrations of EPZ005687 (μM) over the course of five days (half maximal inhibitory concentration value, 20 μM). The results shown depict the optical density on the fifth day of treatment. (B) Immunoblot showing the expression of EZH2 and B7-H3 in D425 and D458 cells (40 μg) treated with 0, 10, or 20 μM of EPZ005687. (C) Scatterplot bar graph depicting EZH2 and B7-H3 protein expression in control and EPZ005687-treated MB cells (24 h). The horizontal black bar represents the median. The vertical black bar represents the SD. *P<0.05 and **P<0.01. EZH2, enhancer of zeste homolog 2; MB, medulloblastoma.

growth of D425 and D458 MB cells treated with increasing concentrations of EPZ005687 was monitored and the results were analyzed after five days of treatment (Fig. 3A). It was found that EPZ005687 decreased the viability of both D425 and D458 cells [half maximal inhibitory concentration (IC_{50}) of 20 μM], in agreement with previous studies (69,70). Notably, it was found that the viability of controls and MB cells treated with higher concentrations of EPZ005687 was reduced to a greater extent than MB cells treated with higher concentrations of Tazemetostat (Fig. S1). While the mechanisms responsible for these observed differences remain to be elucidated, it is possible that the difference in cell viability is attributed to the nature of MB cells used (51). To determine whether pharmacological inhibition of EZH2 also impacted B7-H3 expression, immunoblot analysis of MB cells exposed to increasing concentrations of EPZ005687 was performed. In line with the results obtained from EZH2 knockdown, a reduction in B7-H3 expression was observed with EPZ005687 treatment (Fig. 3B). Treatment with 10 μM or 20 μM of EPZ005687 significantly (P<0.001) downregulated B7-H3 expression in both D425 and D458 cells (Fig. 3C). It was identified that both knockdown of EZH2 and pharmacological inhibition using EPZ005687 led to the downregulation of B7-H3 in MYC-amplified D425 and D458 cells (Figs. 2A and 3B). Since B7-H3 is expressed on the cell membrane as well as intracellularly (71,72), it was next examined how MYC inhibition using JQ1 (1 μM) or EZH2 inhibitors (20 μM) influenced B7-H3 expression by performing flow cytometry on 70% ethanol-fixed D425 cells and stained with PE-labeled B7-H3 antibody (Fig. 4A). It was observed that EPZ005687 treatment reduced B7-H3 expression to a greater extent than control and JQ1-treated MB cells. To further investigate the effects of JQ1 and EPZ005687 on B7-H3 protein expression, immunoblot analysis was performed on D425 and D458 cells, as aforementioned in the 'Materials and Methods' section (Fig. 4B). Statistical analysis revealed that JQ1 and EPZ005687 treatment significantly (P<0.001) reduced EZH2, B7-H3, and MYC protein expression in D425 cells (Fig. 4C). Moreover, EPZ005687 treatment significantly downregulated H3K27me3 (P<0.05) and B7-H3 (P<0.05) expression in D458 cells. Compared with D425 cells, the higher basal protein levels of MYC in D458 cells (24,38) may explain why significant reductions in MYC protein expression were not observed in EPZ005687-treated D458 cells.

EZH2 inhibition downregulates B7-H3 mRNA and is associated with increased miR-29a/b expression. It has been reported that EZH2 directly interacts with MYC and MYCN, with EZH2 depletion resulting in reduced MYC expression and transcriptional activity (38). A similar study revealed that EZH2 and MYC induce each other's expression through miRNA targeting (34). To investigate whether such mechanisms may participate in MB, RT-qPCR analysis was performed on D425 and D458 cells treated with or without EPZ005687 for 24 h. The results demonstrated that in D425

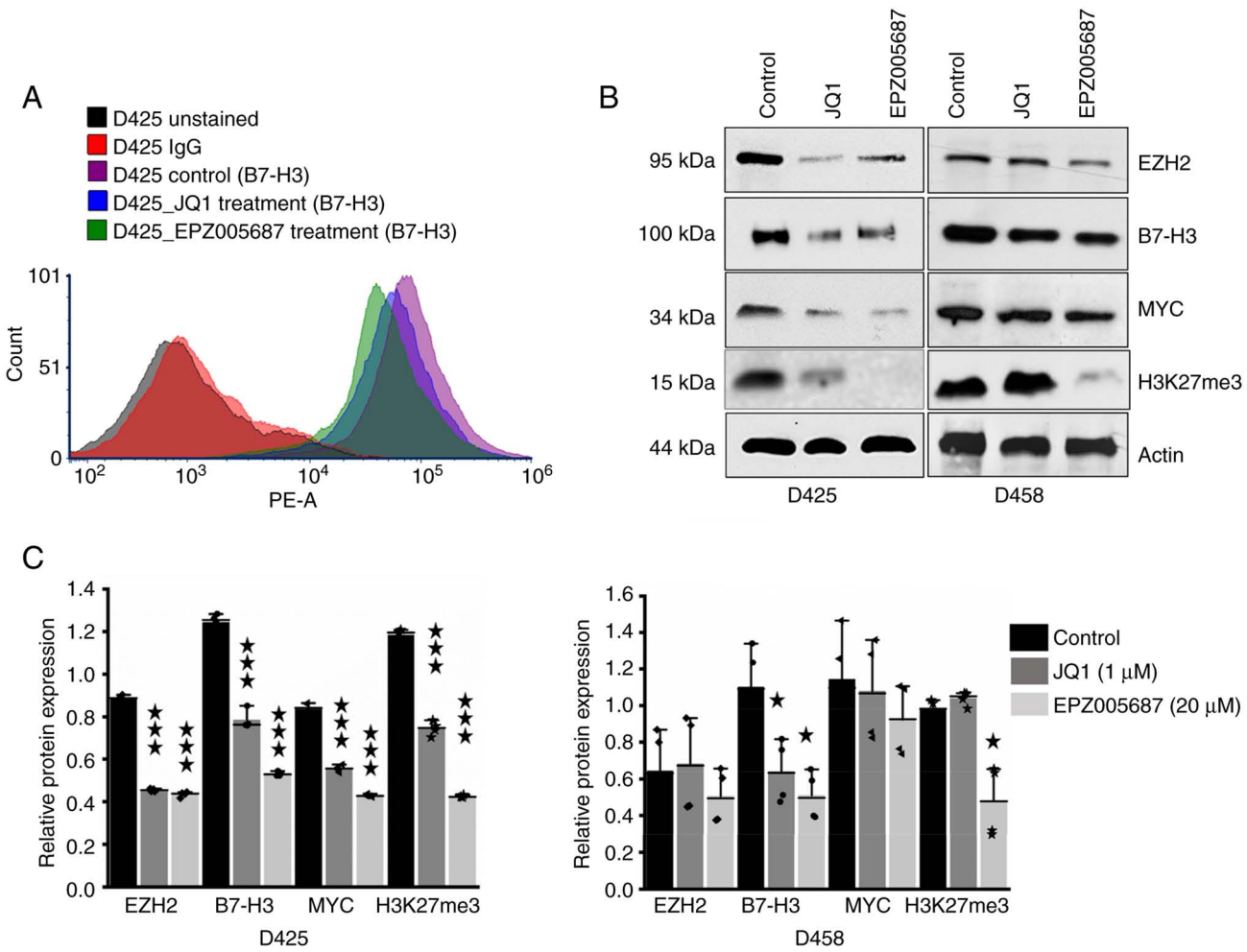

Figure 4. EZH2 inhibition reduces B7-H3 expression. (A) Graph from unstained, PE IgG (2.5 μM), and PE anti-human B7-H3 antibody stained D425 cells treated with JQ1 (1 μM) or EPZ005687 (20 μM). IgG served as the negative control. (B) Immunoblot depicting the expression of EZH2, B7-H3, MYC and H3K27me3 in D425 and D458 cells (40 μg) treated with or without JQ1 (1 μM) and EPZ005687 (20 μM). (C) Scatterplot bar graph of EZH2, B7-H3, MYC and H3K27me3 protein expression in control and treated MB cells. The horizontal black bar represents the median. The vertical black bar represents the SD. *P<0.05 and ***P<0.001. EZH2, enhancer of zeste homolog 2; PE, phycoerythrin.

cells, EPZ005687 treatment significantly reduced the mRNA levels of EZH2 (P<0.001), B7-H3 (P<0.001) and MYC (P<0.01) when compared with controls (Fig. 5A). EPZ005687 treatment also led to significant downregulation of EZH2 (P<0.01) and B7-H3 (P<0.01) mRNA levels in D458 cells (Fig. 5B). These results indicated that EPZ005687 reduces B7-H3 expression in Group 3 MB cells at the post-transcriptional level.

In addition to EZH2 and MYC, miR-29a is known to regulate B7-H3 expression through translational suppression (35,73). Importantly, both EZH2 and MYC can bind to the promoter regions of miR-29a/b1 and miR29b2/c, leading to miR-29 suppression (34). Thus, it stands to reason that EZH2 and MYC may indirectly augment B7-H3 expression through targeting miR-29a/b. This notion is supported by a previous study by the authors which demonstrated that the endogenous levels of miR-29a are low in D425 and D458 cells; However, JQ1 significantly increased miR-29a/b transcript levels, whereas forced expression of miR-29a/b significantly reduced B7-H3 levels (24). As EZH2 inhibition downregulated B7-H3 protein levels (Fig. 3C), it was wondered whether EZH2 may regulate B7-H3 expression indirectly through miR-29a/b suppression. To evaluate this possibility, miR-29a/b expression upon EPZ005687 treatment was assessed. The results from RT-qPCR analysis revealed that in D425 cells, miR-29 transcript levels were significantly (P<0.01) increased following EZH2 inhibition (Fig. 5C). miR-29a/b mRNA levels were also increased in EPZ005687-treated D458 cells (Fig. 5D). As EPZ005687 treatment downregulated B7-H3 protein levels with corresponding increases in miR-29a expression, this suggests that EZH2 inhibition may facilitate miR-29a-mediated B7-H3 suppression.

As revealed in Fig. 4B, both JQ1 and EPZ005687 treatments led to significant reductions in B7-H3 expression. To further validate the role of EZH2 and MYC on B7-H3 suppression, immunoblot analysis was conducted on D458 cells transfected with B7-H3 overexpressing plasmids in the presence or absence of JQ1 or EPZ005687. When compared with controls, B7-H3 expression was reduced in both JQ1-, and EPZ005687-treated B7-H3-overexpressing cells (Fig. 5E). However, B7-H3 expression was significantly (P<0.001) reduced in EPZ005687-treated B7-H3 overexpressing cells (Fig. 5F). Collectively, these results indicate that in Group 3 MB cells, EPZ005687 significantly reduces B7-H3 expression at the translational level, potentially through miR-29a/b suppression.

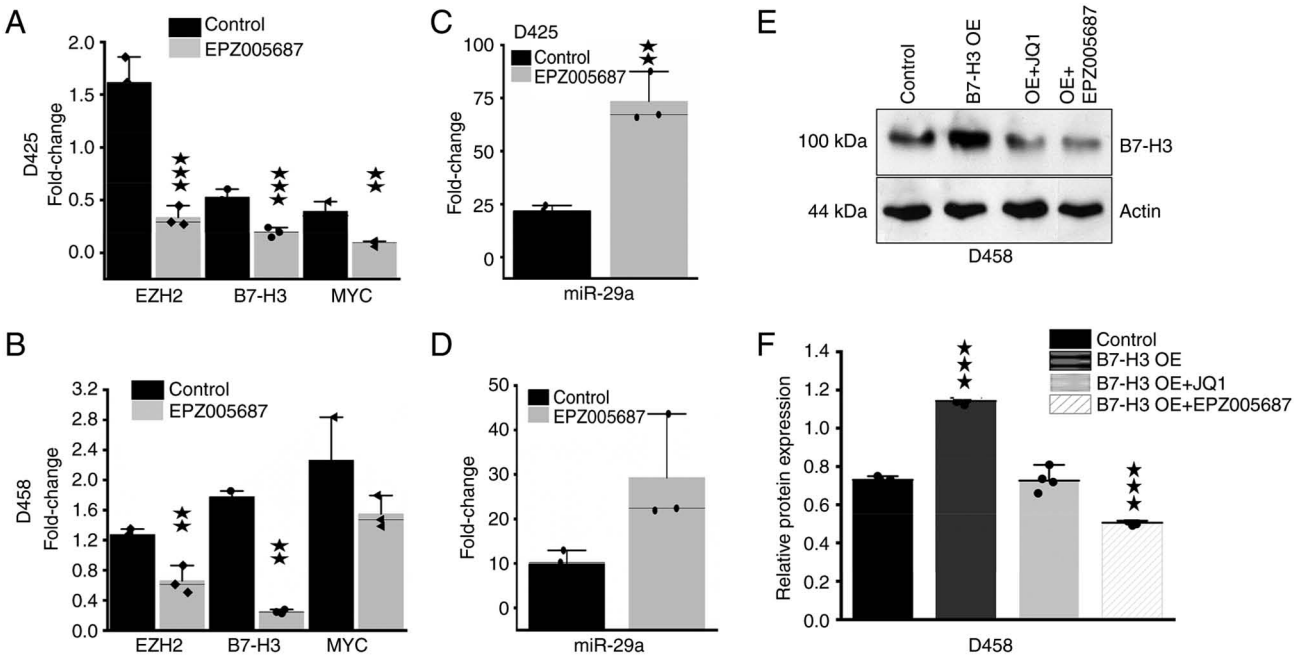

Figure 5. EPZ005687 downregulates B7-H3 and MYC transcript levels and upregulates miR-29 expression. (A and B) Scatterplot bar graph of EZH2, B7-H3, and MYC transcript levels in D425 and D458 cells treated with or without EPZ005687 (20 μM). (C and D) Scatterplot bar graph of miR-29 expression in D425 and D458 cells treated with or without EPZ005687 (20 μM). (E) Immunoblot of D458 cells (40 μg) transfected with B7-H3-OE plasmids (48 h) in the presence or absence of JQ1 (1 μM) or EPZ005687 (20 μM). (F) Scatterplot bar graph of B7-H3 protein expression in control and treated MB cells. The horizontal black bar represents the median. The vertical black bar represents the SD. **P<0.01 and ***P<0.001. miR, microRNA; EZH2, enhancer of zeste homolog 2; OE, overexpressing.

EZH2 inhibition impairs clonogenic survival of Group 3 MYC$^+$ MB cells. As EPZ005687 treatment reduced MB cell viability (Fig. 3A), the effects of MYC and EZH2 inhibition on the MB cell cycle were next compared using flow cytometric analysis. In this experiment, D425 and D458 cells were treated with either JQ1 (1 μM) or EPZ005687 (20 μM) for 24 h. It was found that a significantly greater proportion of D425 cells treated with JQ1 were in the sub-G1 phase when compared with controls (Fig. 6A). Further, EPZ005687 treatment increased the number of D425 cells in the sub-G1 phase, although this difference was not statistically significant. On the other hand, upon EPZ005687 treatment, a significantly greater proportion of D458 cells were in the sub-G1 phase (Fig. 6B), suggesting that EZH2 inhibition promotes cell death in this cell line. Of note, both EPZ005687 and JQ1 treatments appeared to reduce B7-H3 protein levels to a similar degree (Fig. 4C). It is possible that EPZ005687 resulted in a greater proportion of cells in the sub-G1 phase as a result of MYC downregulation (Fig. 5A and B), in addition to B7-H3. However, other mechanisms may be involved.

To examine the long-term impacts of EZH2 inhibition, colony-forming ability in D425 and D458 cells was studied using clonogenic assay. MB cells were plated at densities of 50 and 200 cells and allowed to proliferate over 14 days. Colonies were measured as a cluster of 50 or more cells (Fig. 7A and B). Although both JQ1 and EPZ005687 treatment significantly reduced the number of colonies compared with controls, it was observed that cells treated with EPZ005687 formed fewer visible colonies than those treated with JQ1. Taken together, the present results highlighted the therapeutic potential of EZH2 inhibition in treating aggressive MYC-amplified Group 3 MBs.

EZH2 inhibition downregulates B7-H3 and decreases viability in murine NSCs. MB can be modeled by transforming NSC *in vitro*. The C17.2 murine NSCs are isolated from neonatal mouse cerebellum and immortalized by retroviral-mediated transduction into mitotic progenitor cells (28,39,74). The C17.2 cells are not transformed and do not form tumors in mice, but they grow and transform in the presence of known oncogenes including REST or BMI1 (75) to form tumors with classic MB histology (74). In MB, inhibition of EZH2 significantly attenuates the ability of REST to transform C17.2 cells into tumorigenic stem cells (28), indicating that EZH2 acts as an oncogene in MB as its presence is required for REST-induced transformation (28). Therefore, it was decided to evaluate the role of EZH2 on B7-H3 expression in C17.2 and C17.2 cells that stably overexpress EZH2 (C17.2-EZH2-OE). To determine if EZH2 inhibition impaired NSC viability and whether the drug's efficacy was affected by cells overexpressing EZH2, an MTT assay was performed. C17.2 cells and C17.2-EZH2-OE NSCs were treated with increasing concentrations of EPZ005687. Although both cell lines exhibited an IC_{50} of 20 μM, it was observed that at drug concentrations lower than 10 μM, the C17.2-EZH2-OE cells appeared more sensitive to EPZ005687 treatment when compared with C17.2 cells (Fig. 8A). In addition to higher expression of EZH2 (Fig. 8B), C17.2-EZH2-OE cells also exhibited significantly (P<0.001) higher expression of B7-H3 when compared with C17.2 cells (Fig. 8C). Further, using flow cytometric analysis, it was revealed that a greater percentage of C17.2-EZH2-OE NSCs treated with EPZ005687 were arrested in the G2/M phase when compared with controls (Fig. 8D). Next, the effects of EZH2 inhibition on B7-H3 expression were investigated by

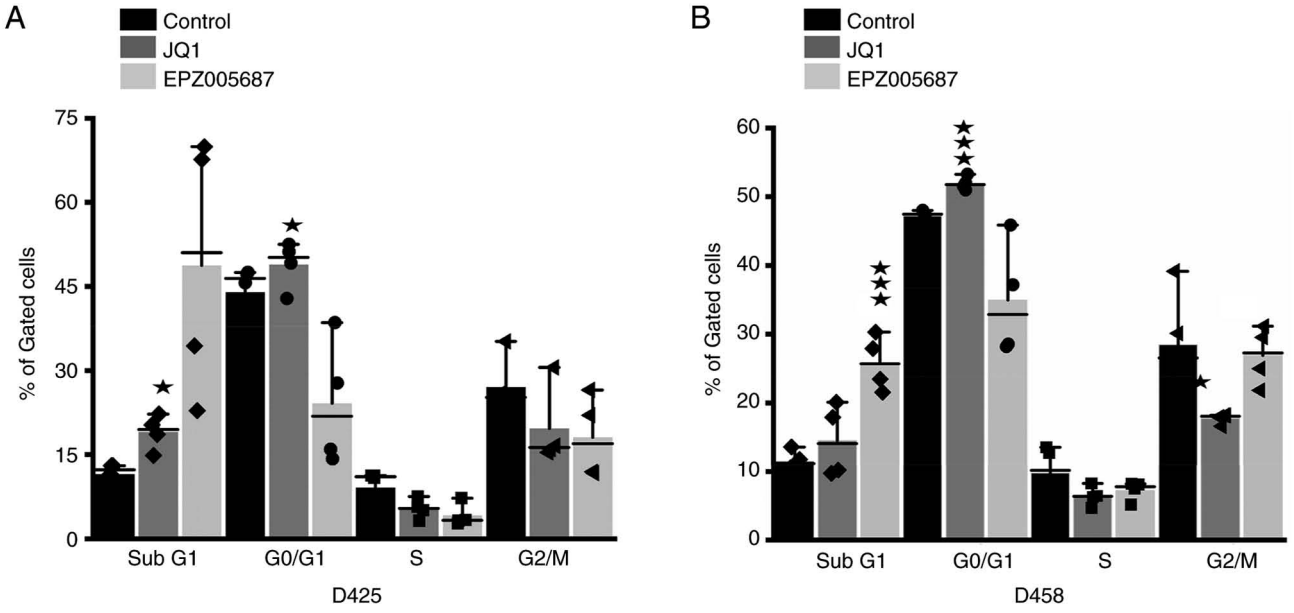

Figure 6. EZH2 inhibition induces sub-G1 arrest in MB cells. (A and B) Cell cycle analysis was performed using flow cytometric analysis of D425 and D458 cells treated with or without JQ1 (1 μM) and EPZ005687 (20 μM) for 24 h. The horizontal black bar represents the median. The vertical black bar represents the SD. *P<0.05 and ***P<0.001. EZH2, enhancer of zeste homolog 2; MB, medulloblastoma.

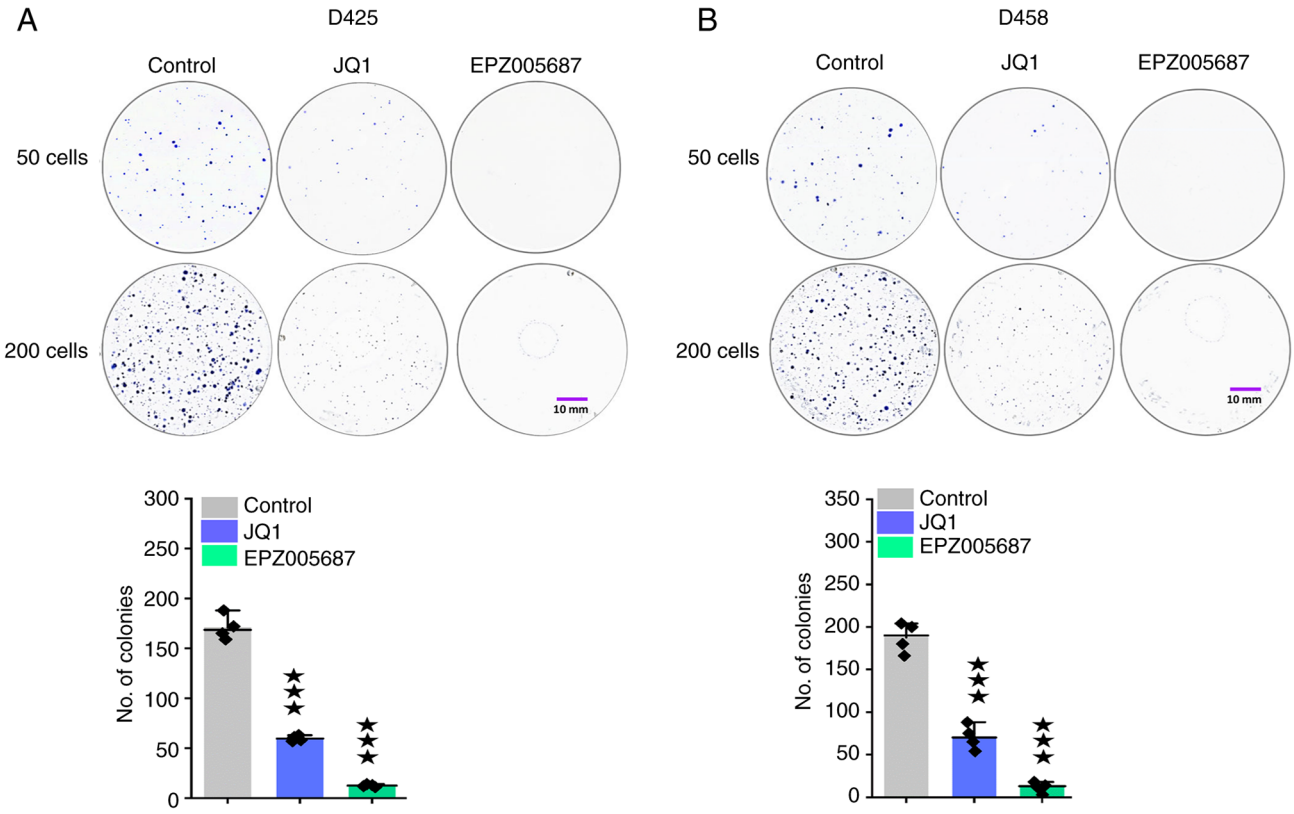

Figure 7. EZH2 inhibition impairs clonogenic survival in MB cells. (A and B) Images captured from the clonogenic assay of control, JQ1-(1 μM), and EPZ005687-(20 μM) treated (A) D425 and (B) D458 cells plated at densities of 50 and 200 cells. The scatterplot bar graphs demonstrate the number of colonies formed over the course of 14 days. The horizontal black bar represents the median. The vertical black bar represents the SD. At 50 and 200 cells, EPZ005687-treated MB cells showed significantly reduced colony-forming ability. ***P<0.001. EZH2, enhancer of zeste homolog 2; MB, medulloblastoma.

immunoblot analysis using C17.2-EZH2-OE NSCs treated with or without EPZ005687. Predictably, EZH2 inhibition significantly (P<0.001) downregulated B7-H3 protein expression (Fig. 8E and F). These results suggest that EZH2 plays a role in regulating B7-H3 expression in NSCs while further supporting the notion that the sensitivity of C17.2-EZH2-OE cells to EPZ005687 is likely the result of higher EZH2-B7-H3 expression. To evaluate this possibility, an MTT assay was

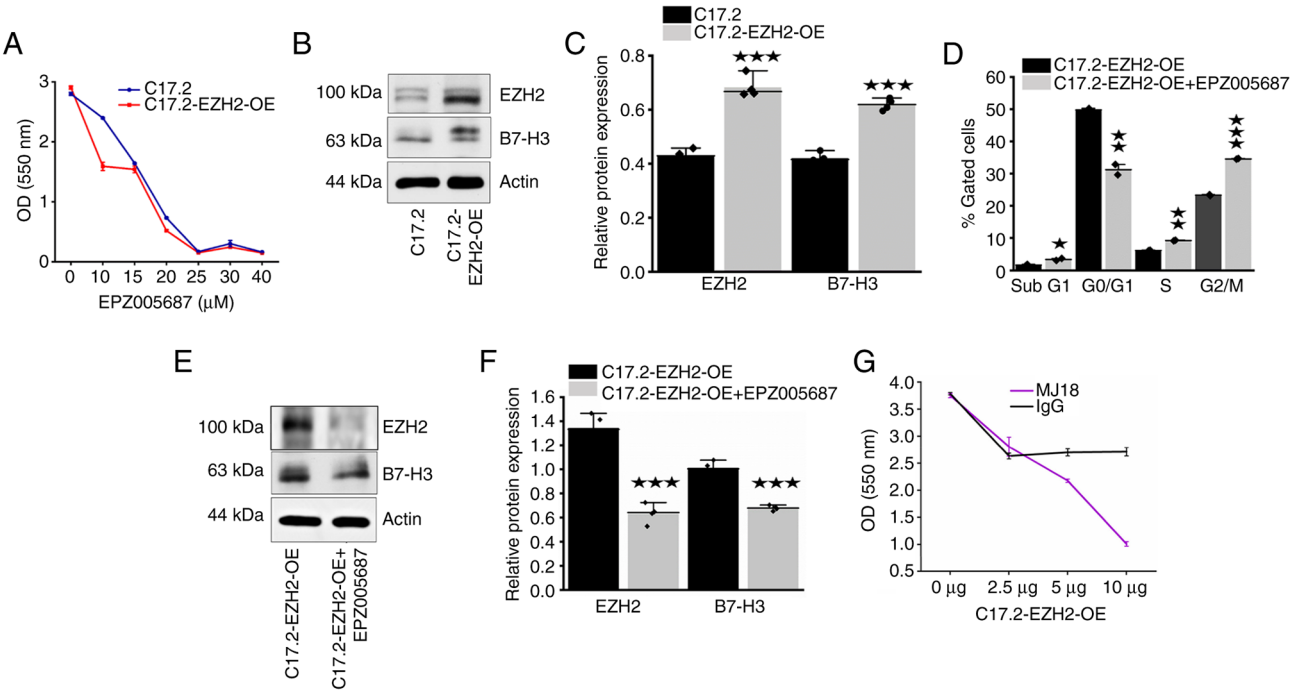

Figure 8. EZH2 inhibition reduces C17.2 NSC viability and downregulates B7-H3 expression. (A) MTT assay (n=10 per cell line) of C17.2 and C17.2-EZH2-OE (NSCs treated with increasing concentrations of EPZ005687 (μM) over the course of five days (half maximal inhibitory concentration value, 20 μM). (B) Immunoblot showing the expression of EZH2 and B7-H3 in C17.2 and C17.2-EZH2-OE NSCs (50 μg). (C) Scatterplot bar graph depicting EZH2 and B7-H3 protein expression in C17.2 and C17.2-EZH-OE NSCs. The horizontal black bar represents the median. The vertical black bar represents the SD. C17.2-EZH2-OE cells exhibited significantly higher levels of EZH2 and B7-H3 when compared with C17.2 NSCs. (D) Flow cytometric analysis of C17.2 and C17.2-EZH2-OE NSCs treated with or without EPZ005687 for 24 h (20 μM). (E) Immunoblot showing EZH2 and B7-H3 protein expression in C17.2 and C17.2-EZH2-OE NSCs treated with or without EPZ005687 (20 μM) for 24 h. (F) EPZ005687 treatment significantly downregulated EZH2 and B7-H3 protein expression. (G) MTT assay on C17.2-EZH2-OE NSCs treated with increasing concentrations of the anti-mouse B7-H3 monoclonal antibody MJ18 or IgG control antibody. *P<0.05, **P<0.01 and ***P<0.001. EZH2, enhancer of zeste homolog 2; OE, overexpressing; NSC, neural stem cell.

conducted on C17.2-EZH2-OE NSCs treated with increasing concentrations of the anti-mouse B7-H3 monoclonal antibody MJ18 or IgG control antibody (76). As observed in Fig. 8G, inhibition of B7-H3 greatly impaired C17.2-EZH2-OE NSC viability.

Discussion

The MYC gene family includes MYC, MYCN and MYCL1 (75). Research has primarily focused on MYC and MYCN, as they are frequently amplified in highly aggressive MBs (75). Notably, the expression of these paralogs differ among the MB subgroups. For instance, amplifications of *MYC*, *MYCN* and *MYCL1* are rare in WNT MB (75). On the other hand, *MYCN* and *MYCL1* are highly expressed in SHH MB. Of note, in Group 3 MB, *MYC* amplifications occur at higher frequency than in any other MB subgroup (13). Finally, Group 4 MBs tend to have low *MYC* and *MYCN* expression when compared with other MB subgroups (75). The functions of MYC in epigenetic regulation have been well described. For example, MYC suppresses miR-29a-c expression likely through direct promoter binding (31). MYC also stimulates EZH2 expression through miR-26a repression (77). Notably, studies in prostate cancer have shown that MYC induces EZH2 expression, with corresponding reductions in both miR-29a and miR-29b (78). Similarly, in acute myeloid leukemia, MYC inhibition is associated with reduced expression of EZH2 mRNA and protein, along with increased miR-29a (79).

The miR-29 family includes miR-29a, miR-29b and miR-29c (32). The three miR-29 isoforms share identical seed sequences, which determines the protein-coding genes a miRNA would target (32). As such, the predicted target genes for miR-29a-c largely overlap. For example, previous studies have revealed that miR-29a directly binds to the 3'-UTR of B7-H3 transcripts to induce translational suppression (35). However, because all three isoforms share the same seed sequence complementarity to the B7-H3 3'-UTR, such findings can also be extended to miR-29b/c (35). For instance, in melanoma, miR-29c directly binds to the 3'-UTR of B7-H3 transcripts (22). The tumor suppressive functions of miR-29 members have been well described (32,35), including Group 3 MB (24). It was previously showed that the endogenous levels of miR-29a are low in D425 and D458 cells (24). However, inhibition of MYC with JQ1 significantly increased miR-29a/b expression, whereas forced expression of miR-29a/b significantly reduced B7-H3 levels (24), indicating that MYC regulates B7-H3 protein expression, in part by suppressing miR-29 levels. In the present study, it was demonstrated that EPZ005687 decreased the protein expression of B7-H3 with concomitant increases in miR-29a expression, suggesting that EZH2 regulates B7-H3 (Fig. 9), in part by miR-29a suppression (35). Future *in vivo* studies are needed to verify the regulation of B7-H3 by the MYC-EZH2-miR-29 axis.

MB is considered to arise from undifferentiated neural stem/progenitor cells found in the external granule layer of the cerebellum (80). In addition to MYC, human MBs

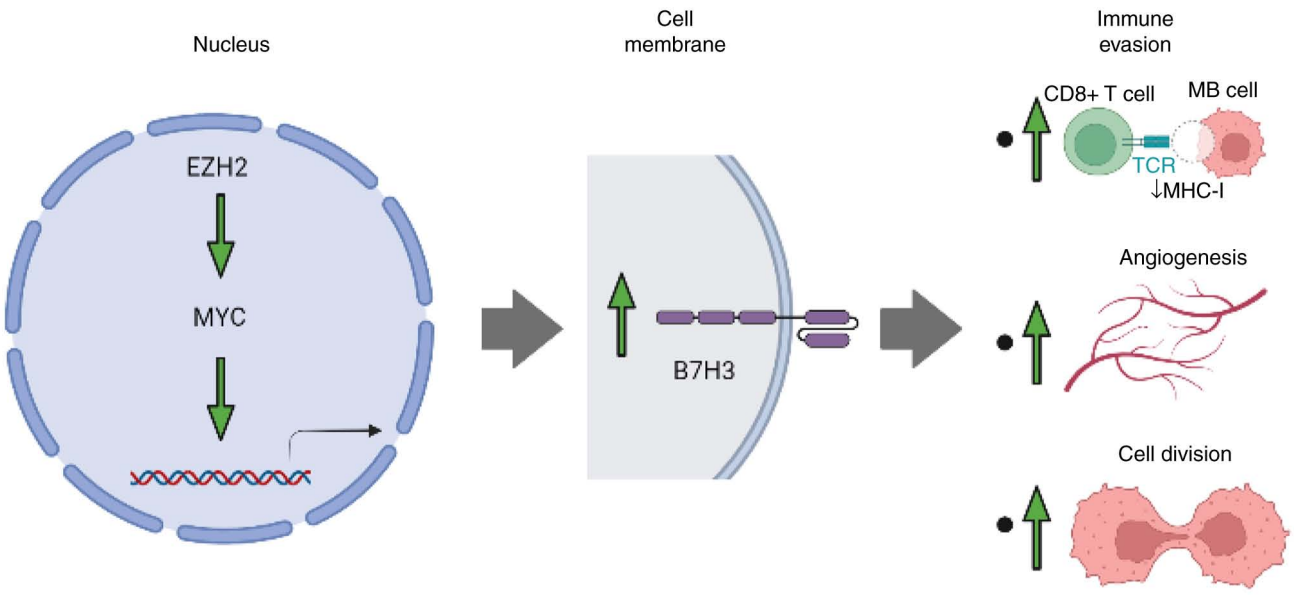

Figure 9. The results of the present study indicate that EZH2 positively regulates MYC to downregulate miR-29a expression in Group 3 MYC+ MB cells. As a result, this leads to the upregulation of B7-H3 protein expression, subsequently promoting immune evasion, angiogenesis and clonogenic survival. EZH2, enhancer of zeste homolog 2.

also express significantly elevated levels of REST/NRSF, a transcriptional suppressor of neuronal differentiation genes (81,82). NSCs transduced with the MYC oncogene do not form tumors in mice because they express the endogenous mouse REST transcripts only under proliferation conditions, which cease upon neuronal differentiation. By contrast, murine NSCs stably expressing c-MYC and transduced with the human REST transgene, continue to express REST/NRSF as they enter neuronal differentiation. This prevents terminal differentiation into mature neurons thereby conferring a proliferative advantage and tumorigenic ability (74). As such, both c-MYC and REST/NRSF overexpression are requirements for NSCs to produce cerebellar tumors. As with other NSC models, C17.2 NSCs do not display anchorage-dependent growth; however, transformation induced by oncogenes such as REST, confers the ability to grow on soft agar (75). In MB, inhibition of EZH2 in REST-transformed C17.2 NSCs impairs their ability to undergo anchorage-dependent growth on soft agar (28), indicating that EZH2 activity is required for this behavior. As such, the C17.2-EZH2-OE NSC line used in the present study serves as a model to test the efficacy of EZH2 inhibition in combating MB tumorigenesis. In the current study, it was found that EPZ005687 treatment significantly reduced the viability of EZH2-amplified NSCs, in addition to downregulating B7-H3 expression, supporting the authors' hypothesis that EZH2 promotes MB tumorigenesis by upregulating B7-H3 expression.

Overexpression of EZH2 was first reported in prostate cancer, with high EZH2 expression being linked with poor patient prognosis (83). Later studies found that EZH2 is also overexpressed in breast, gastric and esophageal cancer, and endometrial carcinoma (84-87), with *EZH2* overexpression being associated with features of aggressive tumor subgroups, clinical progression and reduced survival (84,86). Notably, *EZH2* mRNA is significantly higher in MB tumor tissues when compared with normal tissues (88) and has been proposed as a potential therapeutic target for the treatment of high-risk MB tumors (28). Thus, understanding the oncogenic and regulatory mechanisms of EZH2 has the potential to improve treatment options for a wide range of cancers.

MYC-amplified Group 3 MB is a highly lethal pediatric brain tumor (89,90). Although epigenetic dysregulation is commonly observed in MBs and contributes to their aggressive nature (91,92), fortunately, such epigenetic alterations are reversible (93) with several cancer types including MYC-amplified Group 3 MBs showing success with epigenetic therapy (94,95). The present study sought to evaluate the regulatory role of EZH2 on B7-H3 expression in MYC^+ Group 3 MB *in vitro*. High levels of EZH2 are associated with poor prognosis in MYC-amplified Group 3 MBs. Depletion of EZH2 impaired MB cell viability and clonogenic survival while also reducing B7-H3 and MYC protein expression. A limitation to the present study is the discrepancy observed between B7-H3 expression and cell cycle analysis. Notably, though EPZ005687 and JQ1 treatments appeared to reduce B7-H3 protein levels to a similar degree, a greater proportion of cells treated with EPZ005687 were in the sub-G1 phase than JQ1-treated cells. This suggests that mechanisms other than B7-H3 inhibition are likely involved. Nonetheless, as mutations affecting epigenetic regulators such as EZH2 are frequently reported in Group 3 MBs (14,96,97), the present study highlighted the clinical potential of targeting EZH2 to combat MB pathogenesis. This study further emphasizes the therapeutic potential in targeting EZH2 and B7-H3 in Group 3 MB patients.

Acknowledgements

The authors acknowledge Wade Smith,and Collin Bomstad, (University of Illinois College of Medicine at Peoria (UICOMP), IL, USA) for initiating this work in the lab as a part of the Summer 2018 Craig fellowship program at UICOMP. The

authors also acknowledge Dr. Janardhan Avilala (UICOMP) for his technical assistance. The authors would like to thank UICOMP administrative assistant, Christina Constantinidou for her help with the manuscript formatting.

Funding

The present study was supported by William E. McElroy Charitable Foundation (Springfield, Illinois).

Availability of data and materials

The datasets used and/or analyzed during the current study are available from the corresponding author on reasonable request.

Authors' contributions

SA, IP and KV conceptualized the present study as part of the McElroy grant. SA, KS, IP and SV performed experiments. SA, KV and KS performed the data mining studies. SA and KS confirm the authenticity of all the raw data. SV and RV provided the C17.2 and C17.2-EZH2_OE cells. The methods and materials used in the publication were previously established by SA. All authors contributed to the critical discussions and SA, KS and IP contributed greatly to the analysis of the results. RV made substantial contributions to the conception of the present study and data interpretation. KS and SA wrote the manuscript and IP helped in editing the manuscript. All authors reviewed the manuscript. All authors read and approved the final manuscript.

Ethics approval and consent to participate

Not applicable.

Patient consent for publication

Not applicable.

Competing interests

The authors declare that they have no competing interests.

References

1. Ostrom QT, Gittleman H, Truitt G, Boscia A, Kruchko C and Barnholtz-Sloan JS: CBTRUS Statistical report: Primary brain and other central nervous system tumors diagnosed in the united states in 2011-2015. Neuro Oncol 20 (Suppl_4): iv1-iv86, 2018.
2. Vladoiu MC, El-Hamamy I, Donovan LK, Farooq H, Holgado BL, Sundaravadanam Y, Ramaswamy V, Hendrikse LD, Kumar S, Mack SC, *et al*: Childhood cerebellar tumours mirror conserved fetal transcriptional programs. Nature 572: 67-73, 2019.
3. Hovestadt V, Smith KS, Bihannic L, Filbin MG, Shaw ML, Baumgartner A, DeWitt JC, Groves A, Mayr L, Weisman HR, *et al*: Resolving medulloblastoma cellular architecture by single-cell genomics. Nature 572: 74-79, 2019.
4. Taylor MD, Northcott PA, Korshunov A, Remke M, Cho YJ, Clifford SC, Eberhart CG, Parsons DW, Rutkowski S, Gajjar A, *et al*: Molecular subgroups of medulloblastoma: The current consensus. Acta Neuropathol 123: 465-472, 2012.
5. Ramaswamy V, Remke M, Bouffet E, Faria CC, Perreault S, Cho YJ, Shih DJ, Luu B, Dubuc AM, Northcott PA, *et al*: Recurrence patterns across medulloblastoma subgroups: An integrated clinical and molecular analysis. Lancet Oncol 14: 1200-1207, 2013.
6. Northcott PA, Korshunov A, Witt H, Hielscher T, Eberhart CG, Mack S, Bouffet E, Clifford SC, Hawkins CE, French P, *et al*: Medulloblastoma comprises four distinct molecular variants. J Clin Oncol 29: 1408-1414, 2011.
7. Louis DN, Ohgaki H, Wiestler OD, Cavenee WK, Burger PC, Jouvet A, Scheithauer BW and Kleihues P: The 2007 WHO classification of tumours of the central nervous system. Acta Neuropathol 114: 97-109, 2007.
8. Louis DN, Perry A, Reifenberger G, von Deimling A, Figarella-Branger D, Cavenee WK, Ohgaki H, Wiestler OD, Kleihues P and Ellison DW: The 2016 World Health Organization classification of tumors of the central nervous system: A summary. Acta Neuropathol 131: 803-820, 2016.
9. Eberhart CG, Kratz J, Wang Y, Summers K, Stearns D, Cohen K, Dang CV and Burger PC: Histopathological and molecular prognostic markers in medulloblastoma: c-myc, N-myc, TrkC, and anaplasia. J Neuropathol Exp Neurol 63: 441-449, 2004.
10. Ellison DW, Kocak M, Dalton J, Megahed H, Lusher ME, Ryan SL, Zhao W, Nicholson SL, Taylor RE, Bailey S and Clifford SC: Definition of disease-risk stratification groups in childhood medulloblastoma using combined clinical, pathologic, and molecular variables. J Clin Oncol 29: 1400-1407, 2011.
11. Kool M, Jones DT, Jager N, Northcott PA, Pugh TJ, Hovestadt V, Piro RM, Esparza LA, Markant SL, Remke M, *et al*: Genome sequencing of SHH medulloblastoma predicts genotype-related response to smoothened inhibition. Cancer Cell 25: 393-405, 2014.
12. Millard NE and De Braganca KC: Medulloblastoma: WHO 2021 and beyond. J Child Neurol 31: 1341-1353, 2016.
13. Remke M, Hielscher T, Northcott PA, Witt H, Ryzhova M, Wittmann A, Benner A, von Deimling A, Scheurlen W, Perry A, *et al*: Adult medulloblastoma comprises three major molecular variants. J Clin Oncol 29: 2717-2723, 2011.
14. Pugh TJ, Weeraratne SD, Archer TC, Pomeranz Krummel DA, Auclair D, Bochicchio J, Carneiro MO, Carter SL, Cibulskis K, Erlich RL, *et al*: Medulloblastoma exome sequencing uncovers subtype-specific somatic mutations. Nature 488: 106-110, 2012.
15. Leitner J, Klauser C, Pickl WF, Stöckl J, Majdic O, Bardet AF, Kreil DP, Dong C, Yamazaki T, Zlabinger G, *et al*: B7-H3 is a potent inhibitor of human T-cell activation: No evidence for B7-H3 and TREML2 interaction. Eur J Immunol 39: 1754-1764, 2009.
16. Chapoval AI, Ni J, Lau JS, Wilcox RA, Flies DB, Liu D, Dong H, Sica GL, Zhu G, Tamada K and Chen L: B7-H3: A costimulatory molecule for T cell activation and IFN-gamma production. Nat Immunol 2: 269-274, 2001.
17. Hashiguchi M, Kobori H, Ritprajak P, Kamimura Y, Kozono H and Azuma M: Triggering receptor expressed on myeloid cell-like transcript 2 (TLT-2) is a counter-receptor for B7-H3 and enhances T cell responses. Proc Natl Acad Sci USA 105: 10495-10500, 2008.
18. Chen YW, Tekle C and Fodstad O: The immunoregulatory protein human B7H3 is a tumor-associated antigen that regulates tumor cell migration and invasion. Curr Cancer Drug Targets 8: 404-413, 2008.
19. Han S, Shi X, Liu L, Zong L, Zhang J, Chen Q, Qian Q, Chen L, Wang Y, Jin J, *et al*: Roles of B7-H3 in Cervical Cancer and Its Prognostic Value. J Cancer 9: 2612-2624, 2018.
20. Lin L, Cao L, Liu Y, Wang K, Zhang X, Qin X, Zhao D, Hao J, Chang Y, Huang X, *et al*: B7-H3 promotes multiple myeloma cell survival and proliferation by ROS-dependent activation of Src/STAT3 and c-Cbl-mediated degradation of SOCS3. Leukemia 33: 1475-1486, 2019.
21. Kang FB, Wang L, Jia HC, Li D, Li HJ, Zhang YG and Sun DX: B7-H3 promotes aggression and invasion of hepatocellular carcinoma by targeting epithelial-to-mesenchymal transition via JAK2/STAT3/Slug signaling pathway. Cancer Cell Int 15: 45, 2015.
22. Wang J, Chong KK, Nakamura Y, Nguyen L, Huang SK, Kuo C, Zhang W, Yu H, Morton DL and Hoon DS: B7-H3 associated with tumor progression and epigenetic regulatory activity in cutaneous melanoma. J Invest Dermatol 133: 2050-2058, 2013.
23. Zhong C, Tao B, Chen Y, Guo Z, Yang X, Peng L, Xia X and Chen L: B7-H3 regulates glioma growth and cell invasion through a JAK2/STAT3/Slug-Dependent signaling pathway. Onco Targets Ther 13: 2215-2224, 2020.
24. Purvis IJ, Avilala J, Guda MR, Venkataraman S, Vibhakar R, Tsung AJ, Velpula KK and Asuthkar S: Role of MYC-miR-29-B7-H3 in medulloblastoma growth and angiogenesis. J Clin Med 8: 1158, 2019.

25. Purvis IJ, Velpula KK, Guda MR, Nguyen D, Tsung AJ and Asuthkar S: B7-H3 in medulloblastoma-Derived exosomes; A novel tumorigenic role. Int J Mol Sci 21: 7050, 2020.
26. Loo D, Alderson RF, Chen FZ, Huang L, Zhang W, Gorlatov S, Burke S, Ciccarone V, Li H, Yang Y, *et al*: Development of an Fc-enhanced anti-B7-H3 monoclonal antibody with potent anti-tumor activity. Clin Cancer Res 18: 3834-3845, 2012.
27. Karnell JL, Dimasi N, Karnell FG III, Fleming R, Kuta E, Wilson M, Wu H, Gao C, Herbst R and Ettinger R: CD19 and CD32b differentially regulate human B cell responsiveness. J Immunol 192: 1480-1490, 2014.
28. Alimova I, Venkataraman S, Harris P, Marquez VE, Northcott PA, Dubuc A, Taylor MD, Foreman NK and Vibhakar R: Targeting the enhancer of zeste homologue 2 in medulloblastoma. Int J Cancer 131: 1800-1809, 2012.
29. Pasini D and Di Croce L: Emerging roles for Polycomb proteins in cancer. Curr Opin Genet Dev 36: 50-58, 2016.
30. Simon JA and Lange CA: Roles of the EZH2 histone methyltransferase in cancer epigenetics. Mutat Res 647: 21-29, 2008.
31. Chang TC, Yu D, Lee YS, Wentzel EA, Arking DE, West KM, Dang CV, Thomas-Tikhonenko A and Mendell JT: Widespread microRNA repression by Myc contributes to tumorigenesis. Nat Genet 40: 43-50, 2008.
32. Kriegel AJ, Liu Y, Fang Y, Ding X and Liang M: The miR-29 family: Genomics, cell biology, and relevance to renal and cardiovascular injury. Physiol Genomics 44: 237-244, 2012.
33. Yin H, Wang Y, Wu Y, Zhang X, Zhang X, Liu J, Wang T, Fan J, Sun J, Yang A and Zhang R: EZH2-mediated Epigenetic Silencing of miR-29/miR-30 targets LOXL4 and contributes to tumorigenesis, metastasis, and immune microenvironment remodeling in breast cancer. Theranostics 10: 8494-8512, 2020.
34. Zhang X, Zhao X, Fiskus W, Lin J, Lwin T, Rao R, Zhang Y, Chan JC, Fu K, Marquez VE, *et al*: Coordinated silencing of MYC-mediated miR-29 by HDAC3 and EZH2 as a therapeutic target of histone modification in aggressive B-Cell lymphomas. Cancer Cell 22: 506-523, 2012.
35. Ganju A, Khan S, Hafeez BB, Behrman SW, Yallapu MM, Chauhan SC and Jaggi M: miRNA nanotherapeutics for cancer. Drug Discov Today 22: 424-432, 2017.
36. Italiano A, Soria J, Toulmonde M, Michot JM, Lucchesi C, Varga A, Coindre JM, Blakemore SJ, Clawson A, Suttle B, *et al*: Tazemetostat, an EZH2 inhibitor, in relapsed or refractory B-cell non-Hodgkin lymphoma and advanced solid tumours: A first-in-human, open-label, phase 1 study. Lancet Oncol 19: 649-659, 2018.
37. Morschhauser F, Tilly H, Chaidos A, McKay P, Phillips T, Assouline S, Batlevi CL, Campbell P, Ribrag V, Damaj GL, *et al*: Tazemetostat for patients with relapsed or refractory follicular lymphoma: An open-label, single-arm, multicentre, phase 2 trial. Lancet Oncol 21: 1433-1442, 2020.
38. Zhao Y, Li T, Tian S, Meng W, Sui Y, Yang J, Wang B, Liang Z, Zhao H, Han Y, *et al*: Effective inhibition of MYC-Amplified Group 3 medulloblastoma through targeting EIF4A1. Cancer Manag Res 12: 12473-12485, 2020.
39. Venkataraman S, Birks DK, Balakrishnan I, Alimova I, Harris PS, Patel PR, Handler MH, Dubuc A, Taylor MD, Foreman NK and Vibhakar R: MicroRNA 218 acts as a tumor suppressor by targeting multiple cancer phenotype-associated genes in medulloblastoma. J Biol Chem 288: 1918-1928, 2013.
40. Parker MA, Anderson JK, Corliss DA, Abraria VE, Sidman RL, Park KI, Teng YD, Cotanche DA and Snyder EY: Expression profile of an operationally-defined neural stem cell clone. Exp Neurol 194: 320-332, 2005.
41. Asuthkar S, Velpula KK, Nalla AK, Gogineni VR, Gondi CS and Rao JS: Irradiation-induced angiogenesis is associated with an MMP-9-miR-494-syndecan-1 regulatory loop in medulloblastoma cells. Oncogene 33: 1922-1933, 2014.
42. Asuthkar S, Gondi CS, Nalla AK, Velpula KK, Gorantla B and Rao JS: Urokinase-type plasminogen activator receptor (uPAR)-mediated regulation of WNT/β-catenin signaling is enhanced in irradiated medulloblastoma cells. J Biol Chem 287: 20576-20589, 2012.
43. Asuthkar S, Venkataraman S, Avilala J, Shishido K, Vibhakar R, Veo B, Purvis IJ, Guda MR and Velpula KK: SMYD3 promotes cell cycle progression by inducing cyclin D3 transcription and stabilizing the cyclin D1 protein in medulloblastoma. Cancers (Basel) 14: 1673, 2022.
44. Huang Y, Zhang HL, Li ZL, Du T, Chen YH, Wang Y, Ni HH, Zhang KM, Mai J, Hu BX, *et al*: FUT8-mediated aberrant N-glycosylation of B7H3 suppresses the immune response in triple-negative breast cancer. Nat Commun 12: 2672, 2021.
45. Kim K, Yoo HC, Kim BG, Kim S, Sung Y, Yoon I, Yu YC, Park SJ, Kim JH, Myung K, *et al*: O-GlcNAc modification of leucyl-tRNA synthetase 1 integrates leucine and glucose availability to regulate mTORC1 and the metabolic fate of leucine. Nat Commun 13: 2904, 2022.
46. Li Y, Zhang M, Feng H and Mahati S: The tumorigenic properties of EZH2 are mediated by MiR-26a in uveal melanoma. Front Mol Biosci 8: 713542, 2021.
47. Girault V, Gilard V, Marguet F, Lesueur C, Hauchecorne M, Ramdani Y, Laquerrière A, Marret S, Jégou S, Gonzalez BJ, *et al*: Prenatal alcohol exposure impairs autophagy in neonatal brain cortical microvessels. Cell Death Dis 8: e2610, 2017.
48. Yang L, Li Z and Ouyang Y: Taurine attenuates ER stressassociated apoptosis and catabolism in nucleus pulposus cells. Mol Med Rep 25: e2610, 2017.
49. Asuthkar S, Nalla AK, Gondi CS, Dinh DH, Gujrati M, Mohanam S and Rao JS: Gadd45a sensitizes medulloblastoma cells to irradiation and suppresses MMP-9-mediated EMT. Neuro Oncol 13: 1059-1073, 2011.
50. Zhang G, Xu Y, Lu X, Huang H, Zhou Y, Lu B and Zhang X: Diagnosis value of serum B7-H3 expression in non-small cell lung cancer. Lung Cancer 66: 245-249, 2009.
51. Xu F, Yi J, Wang F, Wang W, Wang Z, Xue J and Luan X: Involvement of soluble B7-H3 in combination with the serum inflammatory cytokines interleukin-17, -8 and -6 in the diagnosis of hepatocellular carcinoma. Oncol Lett 14: 8138-8143, 2017.
52. Wang L, Kang FB, Zhang GC, Wang J, Xie MF and Zhang YZ: Clinical significance of serum soluble B7-H3 in patients with osteosarcoma. Cancer Cell Int 18: 115, 2018.
53. Miele E, Valente S, Alfano V, Silvano M, Mellini P, Borovika D, Marrocco B, Po A, Besharat ZM, Catanzaro G, *et al*: The histone methyltransferase EZH2 as a druggable target in SHH medulloblastoma cancer stem cells. Oncotarget 8: 68557-68570, 2017.
54. Zwergel C, Romanelli A, Stazi G, Besharat ZM, Catanzaro G, Tafani M, Valente S and Mai A: Application of small epigenetic modulators in pediatric medulloblastoma. Front Pediatr 6: 370, 2018.
55. Xu H, Cheung IY, Guo HF and Cheung NK: MicroRNA miR-29 modulates expression of immunoinhibitory molecule B7-H3: Potential implications for immune based therapy of human solid tumors. Cancer Res 69: 6275-6281, 2009.
56. Brown HG, Kepner JL, Perlman EJ, Friedman HS, Strother DR, Duffner PK, Kun LE, Goldthwaite PT and Burger PC: 'Large cell/anaplastic' medulloblastomas: A pediatric oncology group study. J Neuropathol Exp Neurol 59: 857-865, 2000.
57. Leonard JR, Cai DX, Rivet DJ, Kaufman BA, Park TS, Levy BK and Perry A: Large cell/anaplastic medulloblastomas and medullomyoblastomas: Clinicopathological and genetic features. J Neurosurg 95: 82-88, 2001.
58. Liu H, Sun Q, Sun Y, Zhang J, Yuan H, Pang S, Qi X, Wang H, Zhang M, Zhang H, *et al*: MELK and EZH2 cooperate to regulate medulloblastoma cancer stem-like cell proliferation and differentiation. Mol Cancer Res 15: 1275-1286, 2017.
59. Alassiri AH, Alsufiani FM, Almutairi AA, Almohini IA, Aldosari MA and Essa MF: Spectrum of medulloblastoma subtypes and frequency of MYC amplification; Experience from a tertiary care center in Saudi Arabia. Neurosciences (Riyadh) 25: 218-221, 2020.
60. Habib S, Ariatti M and Singh M: Anti-c-myc RNAi-Based Onconanotherapeutics. Biomedicines 8: 612, 2020.
61. Webb MS, Tortora N, Cremese M, Kozlowska H, Blaquiere M, Devine DV and Kornbrust DJ: Toxicity and toxicokinetics of a phosphorothioate oligonucleotide against the c-myc oncogene in cynomolgus monkeys. Antisense Nucleic Acid Drug Dev 11: 155-163, 2001.
62. Gjorgjieva M, Sobolewski C, Dolicka D, Correia de Sousa M and Foti M: miRNAs and NAFLD: From pathophysiology to therapy. Gut 68: 2065-2079, 2019.
63. Zhang H, Zhu D, Zhang Z, Kaluz S, Yu B, Devi NS, Olson JJ and Van Meir EG: EZH2 targeting reduces medulloblastoma growth through epigenetic reactivation of the BAI1/p53 tumor suppressor pathway. Oncogene 39: 1041-1048, 2020.
64. Natsumeda M, Liu Y, Nakata S, Miyahara H, Hanaford A, Ahsan S, Stearns D, Skuli N, Kahlert UD, Raabe EH, *et al*: Inhibition of enhancer of zest homologue 2 is a potential therapeutic target for high-MYC medulloblastoma. Neuropathology 39: 71-77, 2019.
65. Li Z, Takenobu H, Setyawati AN, Akita N, Haruta M, Satoh S, Shinno Y, Chikaraishi K, Mukae K, Akter J, *et al*: EZH2 regulates neuroblastoma cell differentiation via NTRK1 promoter epigenetic modifications. Oncogene 37: 2714-2727, 2018.
66. Duan R, Du W and Guo W: EZH2: A novel target for cancer treatment. J Hematol Oncol 13: 104, 2020.

67. Miranda TB, Cortez CC, Yoo CB, Liang G, Abe M, Kelly TK, Marquez VE and Jones PA: DZNep is a global histone methylation inhibitor that reactivates developmental genes not silenced by DNA methylation. Mol Cancer Ther 8: 1579-1588, 2009.
68. Tan J, Yang X, Zhuang L, Jiang X, Chen W, Lee PL, Karuturi RK, Tan PB, Liu ET and Yu Q: Pharmacologic disruption of Polycomb-repressive complex 2-mediated gene repression selectively induces apoptosis in cancer cells. Genes Dev 21: 1050-1063, 2007.
69. Hubaux R, Thu KL, Coe BP, MacAulay C, Lam S and Lam WL: EZH2 promotes E2F-driven SCLC tumorigenesis through modulation of apoptosis and cell-cycle regulation. J Thorac Oncol 8: 1102-1106, 2013.
70. Cao Z, Wu W, Wei H, Zhang W, Huang Y and Dong Z: Downregulation of histone-lysine N-methyltransferase EZH2 inhibits cell viability and enhances chemosensitivity in lung cancer cells. Oncol Lett 21: 26, 2021.
71. Zhang J, Liu L, Han S, Li Y, Qian Q, Zhang Q, Zhang H, Yang Z and Zhang Y: B7-H3 is related to tumor progression in ovarian cancer. Oncol Rep 38: 2426-2434, 2017.
72. Zhang W, Zhang L, Qian J, Lin J, Chen Q, Yuan Q, Zhou J, Zhang T, Shi J and Zhou H: Expression characteristic of 4Ig B7-H3 and 2Ig B7-H3 in acute myeloid leukemia. Bioengineered 12: 11987-12002, 2021.
73. Wang J, Chen X, Xie C, Sun M, Hu C, Zhang Z, Luan L, Zhou J, Zhou J, Zhu X, *et al*: MicroRNA miR-29a inhibits colon cancer progression by downregulating B7-H3 Expression: Potential molecular targets for colon cancer therapy. Mol Biotechnol 63: 849-861, 2021.
74. Su X, Gopalakrishnan V, Stearns D, Aldape K, Lang FF, Fuller G, Snyder E, Eberhart CG and Majumder S: Abnormal expression of REST/NRSF and Myc in neural stem/progenitor cells causes cerebellar tumors by blocking neuronal differentiation. Mol Cell Biol 26: 1666-1678, 2006.
75. Venkataraman S, Alimova I, Fan R, Harris P, Foreman N and Vibhakar R: MicroRNA 128a increases intracellular ROS level by targeting Bmi-1 and inhibits medulloblastoma cancer cell growth by promoting senescence. PLoS One 5: e10748, 2010.
76. Yamato I, Sho M, Nomi T, Akahori T, Shimada K, Hotta K, Kanehiro H, Konishi N, Yagita H and Nakajima Y: Clinical importance of B7-H3 expression in human pancreatic cancer. Br J Cancer 101: 1709-1716, 2009.
77. Sander S, Bullinger L, Klapproth K, Fiedler K, Kestler HA, Barth TF, Möller P, Stilgenbauer S, Pollack JR and Wirth T: MYC stimulates EZH2 expression by repression of its negative regulator miR-26a. Blood 112: 4202-4212, 2008.
78. Koh CM, Iwata T, Zheng Q, Bethel C, Yegnasubramanian S and De Marzo AM: Myc enforces overexpression of EZH2 in early prostatic neoplasia via transcriptional and post-transcriptional mechanisms. Oncotarget 2: 669-683, 2011.
79. Salvatori B, Iosue I, Djodji Damas N, Mangiavacchi A, Chiaretti S, Messina M, Padula F, Guarini A, Bozzoni I, Fazi F and Fatica A: Critical role of c-Myc in acute myeloid leukemia involving direct regulation of miR-26a and histone methyltransferase EZH2. Genes Cancer 2: 585-592, 2011.
80. Eberhart CG and Burger PC: Anaplasia and grading in medulloblastomas. Brain Pathol 13: 376-385, 2003.
81. Ballas N, Grunseich C, Lu DD, Speh JC and Mandel G: REST and its corepressors mediate plasticity of neuronal gene chromatin throughout neurogenesis. Cell 121: 645-657, 2005.
82. Chen ZF, Paquette AJ and Anderson DJ: NRSF/REST is required in vivo for repression of multiple neuronal target genes during embryogenesis. Nat Genet 20: 136-142, 1998.
83. Varambally S, Dhanasekaran SM, Zhou M, Barrette TR, Kumar-Sinha C, Sanda MG, Ghosh D, Pienta KJ, Sewalt RG, Otte AP, *et al*: The polycomb group protein EZH2 is involved in progression of prostate cancer. Nature 419: 624-629, 2002.
84. Bachmann IM, Halvorsen OJ, Collett K, Stefansson IM, Straume O, Haukaas SA, Salvesen HB, Otte AP and Akslen LA: EZH2 expression is associated with high proliferation rate and aggressive tumor subgroups in cutaneous melanoma and cancers of the endometrium, prostate, and breast. J Clin Oncol 24: 268-273, 2006.
85. Qiu BQ, Lin XH, Ye XD, Huang W, Pei X, Xiong D, Long X, Zhu SQ, Lu F, Lin K, *et al*: Long non-coding RNA PSMA3-AS1 promotes malignant phenotypes of esophageal cancer by modulating the miR-101/EZH2 axis as a ceRNA. Aging (Albany NY) 12: 1843-1856, 2020.
86. Gan L, Xu M, Hua R, Tan C, Zhang J, Gong Y, Wu Z, Weng W, Sheng W and Guo W: The polycomb group protein EZH2 induces epithelial-mesenchymal transition and pluripotent phenotype of gastric cancer cells by binding to PTEN promoter. J Hematol Oncol 11: 9, 2018.
87. Krill L, Deng W, Eskander R, Mutch D, Zweizig S, Hoang B, Ioffe O, Randall L, Lankes H, Miller DS and Birrer M: Overexpression of enhance of Zeste homolog 2 (EZH2) in endometrial carcinoma: An NRG oncology/gynecologic oncology group study. Gynecol Oncol 156: 423-429, 2020.
88. Xue P, Huang S, Han X, Zhang C, Yang L, Xiao W, Fu J, Li H and Zhou Y: Exosomal miR-101-3p and miR-423-5p inhibit medulloblastoma tumorigenesis through targeting FOXP4 and EZH2. Cell Death Differ 29: 82-95, 2022.
89. Roussel MF and Robinson GW: Role of MYC in Medulloblastoma. Cold Spring Harb Perspect Med 3: a014308, 2013.
90. Dhall G, Grodman H, Ji L, Sands S, Gardner S, Dunkel IJ, McCowage GB, Diez B, Allen JC, Gopalan A, *et al*: Outcome of children less than three years old at diagnosis with non-metastatic medulloblastoma treated with chemotherapy on the 'Head Start' I and II protocols. Pediatr Blood Cancer 50: 1169-1175, 2008.
91. Huether R, Dong L, Chen X, Wu G, Parker M, Wei L, Ma J, Edmonson MN, Hedlund EK, Rusch MC, *et al*: The landscape of somatic mutations in epigenetic regulators across 1,000 paediatric cancer genomes. Nat Commun 5: 3630, 2014.
92. Feinberg AP, Koldobskiy MA and Gondor A: Epigenetic modulators, modifiers and mediators in cancer aetiology and progression. Nat Rev Genet 17: 284-299, 2016.
93. Veo B, Danis E, Pierce A, Sola I, Wang D, Foreman NK, Jin J, Ma A, Serkova N, Venkataraman S and Vibhakar R: Combined functional genomic and chemical screens identify SETD8 as a therapeutic target in MYC-driven medulloblastoma. JCI Insight 4: e122933, 2019.
94. Cheng Y, He C, Wang M, Ma X, Mo F, Yang S, Han J and Wei X: Targeting epigenetic regulators for cancer therapy: Mechanisms and advances in clinical trials. Signal Transduct Target Ther 4: 62, 2019.
95. Pei Y, Liu KW, Wang J, Garancher A, Tao R, Esparza LA, Maier DL, Udaka YT, Murad N, Morrissy S, *et al*: HDAC and PI3K antagonists cooperate to inhibit growth of MYC-Driven medulloblastoma. Cancer Cell 29: 311-323, 2016.
96. Robinson G, Parker M, Kranenburg TA, Lu C, Chen X, Ding L, Phoenix TN, Hedlund E, Wei L, Zhu X, *et al*: Novel mutations target distinct subgroups of medulloblastoma. Nature 488: 43-48, 2012.
97. Jones DT, Jäger N, Kool M, Zichner T, Hutter B, Sultan M, Cho YJ, Pugh TJ, Hovestadt V, Stütz AM, *et al*: Dissecting the genomic complexity underlying medulloblastoma. Nature 488: 100-105, 2012.